

Actual Flip Angle Imaging: From 3D to 2D

X. Wu¹, D. K. Deelchand¹, V. L. Yarnykh², K. Ugurbil¹, and P-F. Van de Moortele¹

¹Center for Magnetic Resonance Research, University of Minnesota, Minneapolis, MN, United States, ²Department of Radiology, University of Washington, Seattle, Washington, United States

Introduction: Recently, actual flip angle imaging (AFI) has been introduced as an efficient, fast 3D flip angle (FA) mapping technique (1,2). In some circumstance, a 2D version would be preferable (e.g., 2D Parallel Transmission) since it would require a significantly shorter acquisition time. Although in the original 3D version the FA calculation in AFI (1) does not need to take into consideration the impact of slice profiles, this is however not the case when a 2D slice selective version of the same approach is considered, especially with regard to T1 sensitivity. Therefore, the purpose of this study was to evaluate the properties and feasibility of 2D AFI FA mapping where 2D (instead of 3D) image signals are used for FA calculations, using the equation that was derived for the 3D AFI FA mapping. For this purpose, we performed phantom experiments at 9.4 T, together with simulations, to study the relationship between 2D and 3D AFI FA values for different T1's.

Materials and Methods: In AFI, two 3D images (I1 and I2) are acquired corresponding to two interleaved repetition times (TR1 and TR2 = n TR1). The image ratio ($r = I2/I1$) are used to calculate an actual FA map with $\alpha = \arccos[(rn - 1)/(n - r)]$ [1] (where the T1 dependence of r is removed by a first-order approximation approach). Eq. [1] was used for all FA calculations in this study after needed 2D or 3D image signals were obtained from experiments or simulations. As suggested in (2), we used TR1 = 25 ms and $n = 5$. Additionally, for optimal RF and gradient spoiling in experiments, the incremental RF phase was 35°, and the strong gradient spoiling regime was reached (where the areas of spoiling gradients were 225 and 1125 mT·ms/m during TR1 and TR2 delays, respectively). Note that the validity of Eq. [1] requires image signals to be formed by a common FA, which is satisfied in 3D AFI. However, this requirement is generally not met in 2D AFI because signals in this case are from summation of all transverse magnetizations (M_{xy}) of different FA's through the slice of interest (SOI). As can be easily seen from the slice profile, the FA distribution by a RF pulse typically shows a nonlinear pattern. Therefore, 2D AFI using regular RF pulses is expected to provide incorrect and T1 sensitive FA measurements. Considering that ideal RF pulses generating a uniform FA distribution in slice selection excitation would result in an identical FA measurement in 2D and 3D AFI, the bias in 2D AFI may be reduced using RF pulses with a slice profile close as possible to a square. In order to verify this impact of RF slice profiles on 2D AFI, a gauss and a SLR RF pulse were designed and applied in both 2D and 3D AFI FA mappings. The SLR pulse was calculated for a nominal FA of 10° using the FIR filter design approach (3), and the gauss pulse was generated cutting off a mathematical gaussian curve at the two points whose magnitudes were 1% of the maximum. Both pulses were 3 ms in length. **Experiments:** We used an 8Ch RF Transmit (Tx) 9.4 T human scanner (Varian, USA), fitted with home built 16Ch Receiver board. The FA mapping experiments were conducted using an elliptical 8Ch Transceiver stripline array (4,5) and transmitting through all channels together. In order to study the T1 dependence of 2D FA measurements, two doped water phantoms with different T1 values were utilized. One phantom is a sphere (1.8 L, T1 = 220 ms), and the other a cylinder (1 L, 10 cm in diameter, T1 = 1330 ms). Two TR signals from the SOI were obtained using a modified 2D or 3D gradient echo (GE) pulse sequence. Slice thickness was respectively 2 and 4 mm for the gauss and SLR RF pulses in 2D AFI. Select excitation was also exploited for 3D AFI to reduce the impact of ΔB_0 , where slab thickness = 20 cm for excitation and slice thickness = 1 mm for acquisition. The acquisition time was much shorter in 2D AFI than in 3D AFI (11 s vs 10+ min). Before FA mapping, local B1 phase shim (6) was performed on a central region within the SOI in order to improve Tx B1 efficiency. **Simulations:** Numerical simulations with experimental parameters were performed for slice select excitations in an AFI sequence, assuming ideal RF and gradient spoiling. We utilized the same gradient waveforms generated by the scanner (with rewinders). The nominal FA (for on-resonance isochromats) ranged from 10° to 90° with a step of 5°. For each nominal FA, the distribution of steady-state M_{xy} was simulated with a spatial resolution of 0.05 mm along the slice select direction. Image signals were then obtained by summing complex M_{xy} values within a centered bandwidth of thickness = 40 mm and 1 mm for 2D and 3D AFI's, respectively.

Results: Over the typical FA range of practical interest (from 10° to 90°), the slice profile of the SLR pulse was closer to a square shape than that of the gauss pulse (Fig. 1). The relationship between 2D and 3D AFI FA values was closely matched by our simulations (Fig. 2). As expected, 2D AFI provided different and T1 sensitive FA measurements. This difference and T1 sensitivity were reduced using the SLR pulse with a better slice profile. Interestingly, the difference in FA between 2D and 3D AFI's increased with T1.

Conclusions and Discussion: In this study, FA mapping based on 2D AFI has been studied and characterized to some extent using experiments and simulations. Although the measured FA maps within the SOI by 2D AFI presented global patterns similar to those by 3D AFI, the 2D AFI gave deviated FA values from the nominal ones due to the RF pulse profile. Our results also indicate that the FA bias (including T1 sensitivity) of 2D AFI can be reduced by optimizing the RF slice profile over the FA range of interest.

References: 1. V. Yarnykh, MRM 57:192-200(2007). 2. V. Yarnykh, ISMRM 2008, p 3090. 3. J. Pauly, et al., IEEE TMI 10:53-65(1991). 4. G. Adriany et al., MRM 53:434-45(2005). 5. Vaughan et al. MRM 56:1274-82(2006). 6. P-F. Van de Moortele, et al., MRM 54:1503-1518(2005). **Acknowledgments:** KECK Foundation. NIH: EB006835, PAR-02-010, EB007327, P41 RR008079 and P30 NS057091.

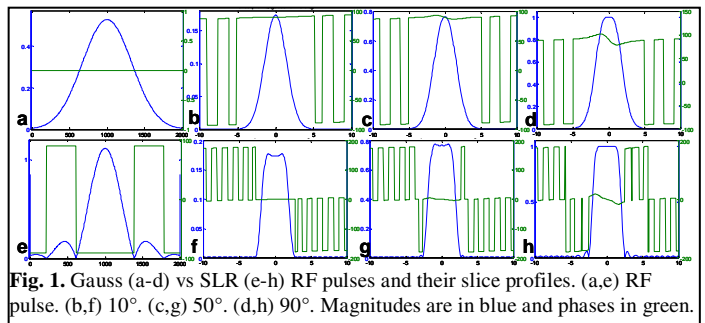


Fig. 1. Gauss (a-d) vs SLR (e-h) RF pulses and their slice profiles. (a,e) RF pulse. (b,f) 10°. (c,g) 50°. (d,h) 90°. Magnitudes are in blue and phases in green.

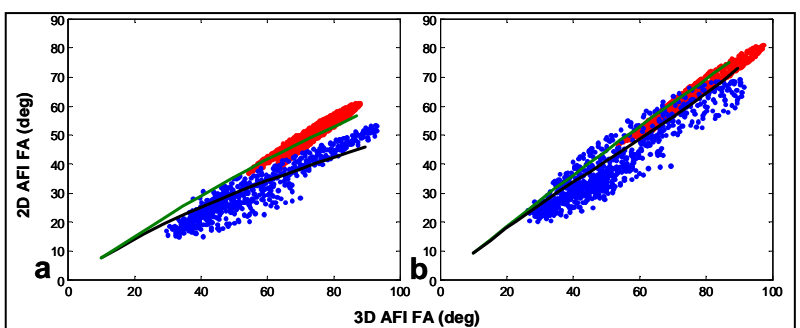


Fig. 2. 2D vs 3D AFI FA using gauss (a) and SLR (b) RF pulses, based on experiments (dots) and simulation (lines) with T1 = 220 (red and green) and 1330 (blue and black) ms.